Degradation of Multistranded Polymers: Effects of Interstrand Stabilization in Xanthan and Scleroglucan Studied by a Monte Carlo Method

Bjørn T. Stokke,*,† Bjørn E. Christensen,‡ and Olav Smidsrød‡

Norwegian Biopolymer Laboratory, Department of Physics and Mathematics and Division of Biotechnology, University of Trondheim, NTH, N-7034 Trondheim, Norway

Received May 14, 1991; Revised Manuscript Received December 4, 1991

ABSTRACT: The depolymerization of double-stranded xanthan and triple-stranded scleroglucan is simulated using a Monte Carlo method. Chain scissions are introduced randomly in each strand to simulate chemical degradation. The cooperative single- to double- or single- to triple-stranded conformational change requires that the chain length exceeds a lower critical value which is incorporated in the model. The simulations show that degradation of such polymers deviates significantly from that of single-stranded polymers. There is initially an apparently enhanced stability where scission of the glycosidic linkages is effectively masked because of interstrand stabilization. This period is followed by a power law region, $M_w \sim t^{-\nu}$, where the exponent ν for a monodisperse starting material is observed to be 1.0, 1.66 ± 0.06, and 2.3 ± 0.1 for the single-, double-, and triple-stranded cases, respectively. Exponents larger than 1 originate from the unmasking of preexisting broken glycosidic linkages when additional scissions are introduced. Analysis of the data reported for the acid-catalyzed degradation of xanthan in the ordered conformation yielded ν = 1.5 ± 0.1, in good agreement with the prediction for a double-stranded model.

Introduction

Dilute and semidilute aqueous solutions of the biopolymers xanthan and scleroglucan are currently used or under development for polymer flooding of oil reservoirs. Polymer additives are used to increase the viscosity and thereby optimize the mobility ratio between the injected fluid and displaced oils in such operations. One major limitation at high temperature has been the loss of viscosity during the flooding process.[1] There are numerous reports on the stability of aqueous xanthan solutions using accelerated tests.[2-8] Identification of one prevalent degradation mechanism as oxidative–reductive depolymerization (ORD), catalyzed by free radicals,[9] has led to the use of antioxidant additives.[9,10] Analogous, acid-catalyzed hydrolysis of the glycosidic linkages can be retarded by controlling the pH,[11] and possible biologically catalyzed depolymerizations can be inactivated adding biocides.[12,13] A third effect that is utilized in stabilizing aqueous xanthan solutions is the enhanced thermal stability of the spectroscopically detected ordered conformation as compared to the disordered conformation.[11,14,15] Thus, formulations including salt concentrations increasing the transition temperature can be utilized to stabilize this biopolymer.

The aim of the present study is to analyze implications of the cooperatively stabilized ordered conformation for stability toward degradation of aqueous xanthan and scleroglucan solutions. The description is valid for degradation where glycosidic linkages are broken randomly and independently in each strand. It is not valid for processes inducing simultaneous adjacent scissions in the two or three strands, as, for instance, in strong elongational shear fields. The enhanced stability of xanthan solutions in the ordered compared to the disordered conformation can be interpreted in terms of a double-helical ordered conformation and a disordered conformation that is at least partly single-stranded.[15-17] Observed degradation rates upon acid-catalyzed depolymerization of xanthan have been explained on the basis of a double-stranded structure.[18] The interpretation was adopted from a model proposed to describe the kinetics of enzymatically catalyzed depolymerization of DNA.[19] The basic idea is that chain scissions must occur in both strands with the relative location not exceeding a certain distance, h, if the double-stranded structure should break into individual species. Parameter h corresponded to two base pairs for the best fit between the calculations and the experimental data of the degradation of the DNA duplex.[19] Hagen[20] likewise reported an h-parameter of 3.5 based on radiation-induced chain scission of native DNA. The ability to form a multistranded conformation is expected to depend on the chain length for low molecular weights. Analysis of the cooperative transition predicts a distribution of the minimum length needed for stabilizing the multistranded conformations. This information is subsequently incorporated into Monte Carlo simulations of the degradation of the double- and triple-stranded polymers. The model predictions will be tested against available experimental data. Last, potential consequences of using the viscosity half-life in a first-order kinetic model of the viscosity decay in simulations of polymer flooding will be discussed.

Effect of Finite Chain Length on the Conformational Transition of Xanthan and Scleroglucan

The cooperative transition from the ordered to the disordered conformation in xanthan can be experimentally detected using various spectroscopical methods, i.e., optical rotation, circular dichroism, or nuclear magnetic resonance. It is generally accepted that the spectroscopically detected conformational transitions reflect a structural transition accompanying changes in long-term thermal stability.[11,14,15] There is ample evidence that the ordered conformation of xanthan is a double-stranded structure[21-26] and that the disordered conformation is at least partly single-stranded.[16,17] The dependence of the transition on the supporting electrolyte[27,28] and the level of acetate and pyruvate substitution[29-31] has been reported. The experimental data reported by Liu and Norisuye[32] suggest that the ordered conformation of xanthan is destabilized by

* Author to whom all correspondence is addressed.
† Department of Physics and Mathematics.
‡ Division of Biotechnology.

0024-9297/92/2225-2209$03.00/0

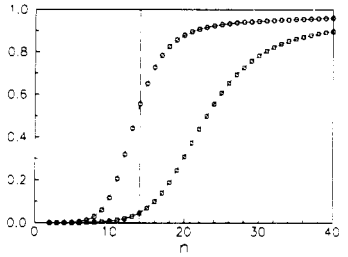

Figure 1. Calculated fraction of intermolecular bonds, f (eq 1), in pairwise associating oligomers versus the degree of polymerization n at T = 30 °C (○) and 70 °C (□) for a hypothetical association characterized by $\gamma = 10^{-5}$, ΔH = 7.5 kJ mol^{-1}, and T_m = 135 °C. Step-function approximation of the transition occurring at n_{min} (- - -).

reduction of the chain length. Thus, at least qualitatively, this links finite chain-length effects to the cooperative transition in xanthan.

The melting of the triple-helical structure of schizophyllan, a polysaccharide of equal chemical composition and a three-dimensional structure like scleroglucan, is reported to occur at about 135 °C in distilled water.[33] The cooperativity in this triple-helix to random-coil transition has been experimentally characterized using differential scanning calorimetry.[34] Moreover, the triple-helical structure existing for weight-average molecular weights $M_w > 12 \times 10^4$ was reported to be destabilized when M_w was reduced, ending up in the single-stranded conformation for M_w less than 4×10^4.[35]

Thus, experimental data both for xanthan and schizophyllan possess signatures of a cooperative transition, and reduction of the molecular weight destabilizes the ordered conformation. In the simulation, we will implement the effect of the final chain length on the stability of the multiple-stranded structures assuming that the chain–chain interactions are intact if consecutive chain scissions are more than n_{min} residues apart (Figure 1). There exist, however, statistical models that describe the pairwise chain–chain association in double- and triple-stranded polymers.[36-39] Consideration of such models may provide additional insight into, e.g., how temperature may affect n_{min} and will therefore be shortly considered. The nonstaggered zipper model of Applequist and Damle[37] specifies the fraction of the number of intermolecular bonds, f, in a pairwise associating oligomer of length N:

$$f(N,s) = \frac{s(1 + 4\gamma J(s) - (1 + 8\gamma J(s))^{1/2})J'(s)}{4\gamma N[J(s)]^2} \quad (1)$$

In eq 1, $J(s)$ equals K/β where K is the equilibrium constant for the pairing reaction, s is the equilibrium constant for elongation of consecutive existing bonds with one additional bond, β is the equilibrium constant for initiating the first bond between two oligomers, $J'(s)$ is a derivative of $J(s)$, and γ is a concentration parameter, $\gamma = \beta c$, where c is the total molar concentration of the oligomers. Parameter β takes into account the initial entropy loss associated with the loss of the independent diffusibility on formation of the first bond. The propagation constant s depends on the actual temperature relative to the transition temperature, T_m, of an infinitely long duplex and the enthalpy change ΔH associated with the interactions. Calculation of f vs N for given γ, ΔH, T_m, and T indicates a sigmoid transition from $f = 0$ to $f = 1$ (Figure 1). The value of N at the midpoint of the transition, $N_{f=0.5}$, increases both as T approaches T_m and as γ decreases. This indicates that n_{min} increases as T approaches T_m. Analogous destabilization of the ordered sequences as the total chain length is reduced is also inherent in the one-sequence model.[40] The theory of Applequist and Damle[37] has been extended and applied to the interpretation of light-scattering data obtained on xanthan through the conformational transition,[41] but it is noticed that the predicted complete strand separation well above T_m still remains to be experimentally validated in xanthan. Although the above theory was developed with pairwise associating polymers in mind, analogous destabilization of the triple-helical structure because of reduction of the chain length can be expected in an appropriate formulation. The experimentally detected destabilization of the triplex structure when the chain length was reduced[35] can be tested in such models, realizing that two bonds can be sufficient to triple the molecular weight and that consideration of the distribution of f is necessary to calculate the average M_w for a given N.

Monte Carlo Simulation of the Degradation of Xanthan and Scleroglucan

In the following, the Monte Carlo approach implemented to gain insight into the effects of the mutual interstrand stabilization of double- and triple-stranded polymers will be described. The description is carried out with xanthan and scleroglucan in mind but is also valid for other double- or triple-stranded polymers stabilized by noncovalent bonds between their strands. We assume that there is a constant catalytic activity toward cleavage of the main-chain glycosidic linkages throughout the degradation and along each chain. The parameter DP refers initially to the degree of polymerization of each of the two or three strands comprising the structure. Inherent in the above assumption is that the side chains and possible changes in those do not affect the catalytic activity toward main-chain cleavage. This may not be well satisfied when the side chains of xanthan are truncated before a major change is observed in the apparent weight-average degree of polymerization.[18]

The simulated depolymerization will be presented as a function of a reduced time, t_r, related to the actual time by a constant depending on the catalytic activity, i.e., determined by the temperature and concentrations of the involved chemicals. In each t_r interval, one of the two or three strands is randomly selected, and then a glycosidic linkage between the first and last linkage is selected. When the selected linkage still is intact, it is broken with a specified probability, α, whereas no action is invoked if previously cleaved. The parameter α is introduced for later use in the incorporation of differences in the catalytic activity in ordered and disordered conformations. The parameter α is set constant, selected to be 0.76 throughout this study as a compromise between getting good resolution in data points at a low degree of depolymerization and not being too computing time intensive. The interstrand interactions are implemented by approximating the cooperative transition, with a step function occurring at the integer n closest to $f = {}^1/_2$ (dotted line in Figure 1). The associated number of repeating units is n_{min} which is converted to the number of main-chain sugar residues by $DP_{min} = 2n_{min}$ based on the repeating unit of xanthan[42] and by $DP_{min} = 3n_{min}$ based on the repeating unit of scleroglucan.[43] Parameter DP_{min} is equivalent to the parameter denoted h by Thomas.[19] The cooperative transition and the experimental data indicate a distribution of DP_{min} (Figure 1), which would correspond to a weighted average over the results presented here for a given DP_{min}. No further action is incorporated when the distance between two nearby scissions either in the same or in adjacent

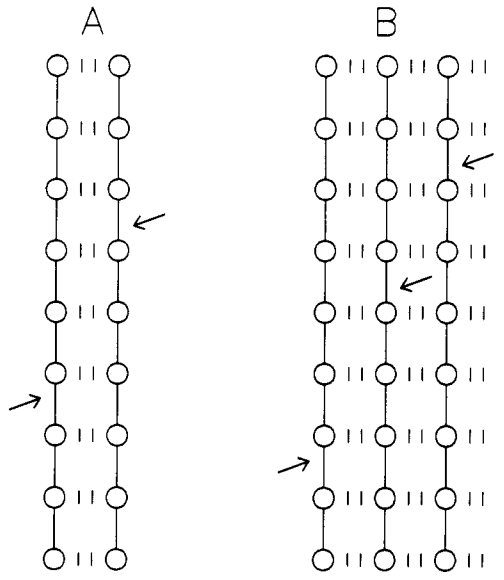

Figure 2. Schematic illustration of the depolymerization of double-helical xanthan (A) and triple-helical scleroglucan (B). Each main-chain residue is denoted as O, the interstrand interactions as ||, and the glycosidic linkages as |. If two scissions (arrows) occur in alternate strands with a mutual separation less than the critical length needed for stabilizing the double helix, a scission of the double strand is induced (A). Simultaneous cleavage (arrows) of the three strands with a relative lateral location less than the critical length is necessary to induce a scission of the triple helix (B).

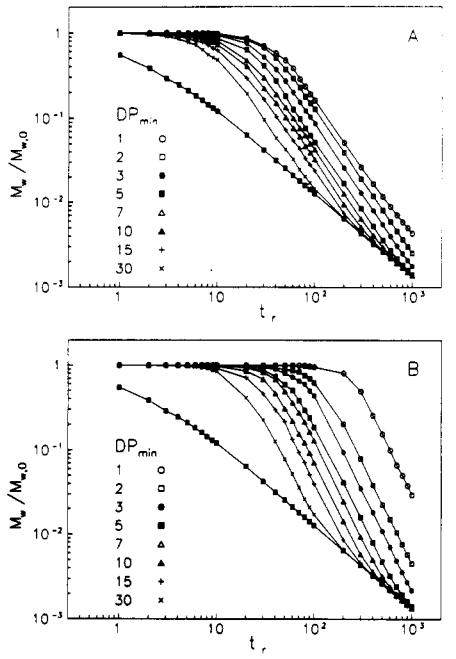

Figure 3. Logarithm of $M_w/M_{w,0}$ versus the logarithm of reduced time for model monodisperse double-stranded (A) and triple-stranded (B) polymers with an initial DP = 1000. The mutual interstrand stabilization was considered for DP_{min} in the range 1–30 as depicted. Random depolymerization of single-stranded polymers (□) is included for comparison.

strands is larger than DP_{min}. When the relative distance is less or equal to DP_{min}, the interstrand interactions are no longer active (Figure 2). This may yield either a scission of the double strand in the case of xanthan when the two scissions are in the separate strands (Figure 2) or an oligomeric species with maximum size DP_{min} (of main-chain residues) when the two scissions occur in the same strand and there is no previous scission in the adjacent strand. Single strands up to $2(DP_{min} - 1)$ can be released with the simultaneous release of oligomers and cleavage of the double- or triple-stranded structure (see also the Results and Discussion section). Scissions in each of the three strands must occur with relative lateral locations less than DP_{min} if a scission of the triple helix should occur (Figure 2).

The number- and weight-average molecular weights, M_n and M_w, of the double- or triple-stranded as well as the single-stranded species are then calculated. These averages are also calculated for the blend of the single and the duplexes or triplexes resulting from the degradation. Molecular weight distributions of degraded samples could optionally be generated. For an idealized, monodisperse starting material, the calculated running average M_n and M_w of the depolymerizing samples were found to converge within 1% at a given t_r when the number of molecules in the ensemble exceeded 50. The initial degree of polymerization was selected between 500 and 3000.

Results and Discussion

Model Predictions. Figure 3 shows a plot of log ($M_w/M_{w,0}$) versus log t_r for an idealized monodisperse xanthan (Figure 3A) and scleroglucan (Figure 3B) with DP = 1000 and DP_{min} ranging from 1 to 30. The initial molecular weight is denoted as $M_{w,0}$. Results from the simulation of random chain scission of the single-stranded polymer is shown for comparison in both the double- and triple-stranded cases. Except in the very early stages, log ($M_w/M_{w,0}$) for the random chain scission of the single-stranded polymer is well represented by a power law dependence on t_r with exponent ν throughout the degradation:

$$M_w/M_{w,0} \sim t_r^{-\nu} \quad (2)$$

The exponent ν is experimentally determined to be 1 for single-stranded polymers, which is in agreement with the analytically deduced relationships for single-stranded polymers.[44]

The simulations on xanthan and scleroglucan depart significantly from the single-stranded polymer in several aspects. Depolymerization of the double- and triple-stranded cases can be divided into three phases. First there is an initial plateau with virtually no change in the apparent M_w, followed by a transition toward a power law region with a larger exponent ν than for the single-stranded polymer. Finally there is a second transition region where $M_w/M_{w,0}$ of the degrading multistranded polymers approaches that for the single-stranded case. The intercept between the extrapolation of the power law region and $M_w/M_{w,0} = 1$ will be referred to as the induction period, $t_{r,ind}$. The exponent in the power law dependence of $M_w/M_{w,0}$ vs t_r in the second power law region is denoted ν_2; i.e., $M_w/M_{w,0} \sim t_r^{-\nu_2}$ for $t_{r,ind} < t_r < t_{r,s}$ where $t_{r,s}$ is used for the reduced time at the transition to the single-stranded degradation kinetics.

Figure 4 shows the induction period $t_{r,ind}$ (Figure 4A) and exponent ν_2 (Figure 4B) versus DP_{min} for double- and triple-stranded polymers with a degree of polymerization DP = 1000. A noticeable and obvious feature is that $t_{r,ind}$ depends strongly on DP_{min} for a given chain length (Figures 3 and 4A). The shorter the number of interstrand interactions needed to keep the double or triple strand intact, the longer the induction period. For instance, the induction period for a double strand with DP = 1000 is 30 at $DP_{min} = 2$, which reduces to 20 at $DP_{min} = 4$. The induction period is also longer for the triple-stranded polymer than for the double-stranded polymer for a given DP_{min} (Figures 3 and 4A). The exponents ν_2 are inde-

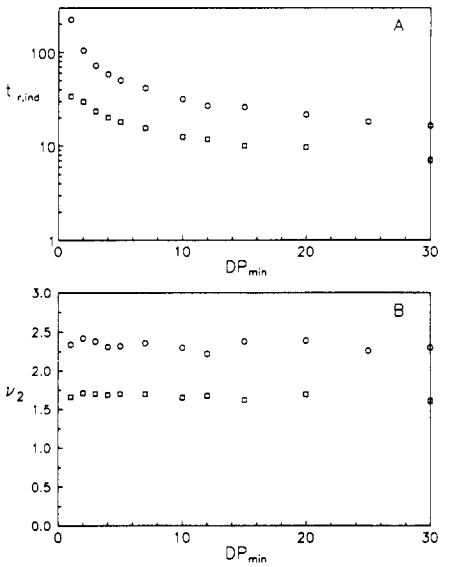

Figure 4. Length of the induction period (A) and exponent ν_2 (B) versus DP_{min} for depolymerization of idealized monodisperse xanthan (□) and scleroglucan (○). The initial degrees of polymerization were in both cases 1000.

pendent of DP_{min} with average values 1.66 ± 0.06 and 2.3 ± 0.1 for the double- and triple-stranded polymers, respectively (Figure 4B). Scission of one covalent bond within a single-stranded polymer molecule yields *two* independent species and corresponds to a coefficient $\nu = 1$. The observed ν_2 for double- and triple-stranded polymers imply that additional scissions of one covalent bond increase the number of species by factors of 2.7 and 3.3, respectively. The apparent depolymerization is therefore faster for the multistranded polymers than for the single-stranded ones for $t_{r,ind} < t_r < t_{r,s}$.

Figure 5 illustrates the consequences of scission of one additional glycosidic linkage: (A) the double-stranded species is intact after cleavage of one glycosidic linkage; (B) scission of a glycosidic linkage that results in two independent species either by release of a single-stranded oligomer or (C) by scission of the double-stranded structure. The fourth possibility (D) that scission of one glycosidic linkage yields three independent species occurs by releasing a single-stranded oligomer while simultaneously inducing a scission of the double strand or, if occurring close to the end of the polymer, by releasing two single-stranded fragments (not shown). Throughout the degradation these events occur simultanously. Event A is dominating when the average length between preexisting broken linkages is large compared to DP_{min}, i.e., $t_r < t_{r,ind}$, whereas types B–D are more prevalent for $t_r > t_{r,ind}$.

Analogous events in the triple-stranded case are illustrated schematically in Figure 6. The type of scission which does not change the number of independent species is not illustrated since it is analogous to that for the double-stranded case. Cleavage of glycosidic linkages yielding two independent species either by release of a single-stranded fragment or by scission of the triple helix is illustrated in A and B, respectively. Examples illustrating three and four freely diffusing species resulting from cleavage of one glycosidic linkage are shown in C and D, respectively. As the degradation proceeds, the dominating events change from that in Figure 6A occurring mainly for $t_r < t_{r,ind}$ to types illustrated in parts B–D of Figure 6 dominating for $t_r > t_{r,ind}$.

The independence of ν_2 on DP_{min} within the double- and triple-stranded polymers and the correlation between ν_2 and strandedness for high molecular weight polymers

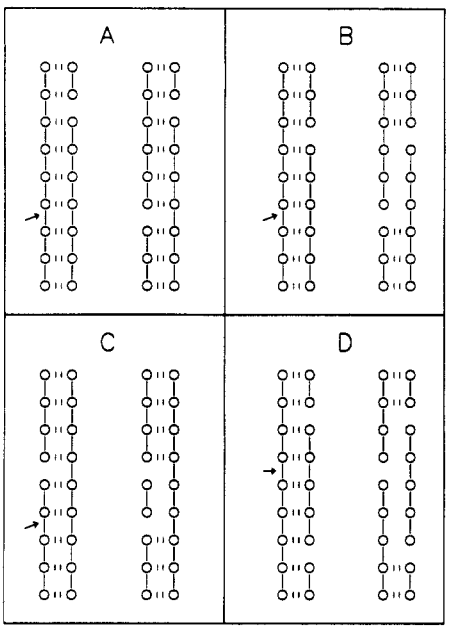

Figure 5. Schematic illustration of the consequences of cleavage (arrow) of a glycosidic linkage in one of the strands in a double-stranded species: scission resulting in no change in the number of species (A), scission resulting in two species either by release of an oligosaccharide shorter than DP_{min} (B) or by scission of the double strand when a neighboring preexisting nick is less than DP_{min} apart (C), and scission resulting in three independent species by simultaneous release of an oligosaccharide and double-strand scission (D). $DP_{min} = 4$ was assumed in this illustration.

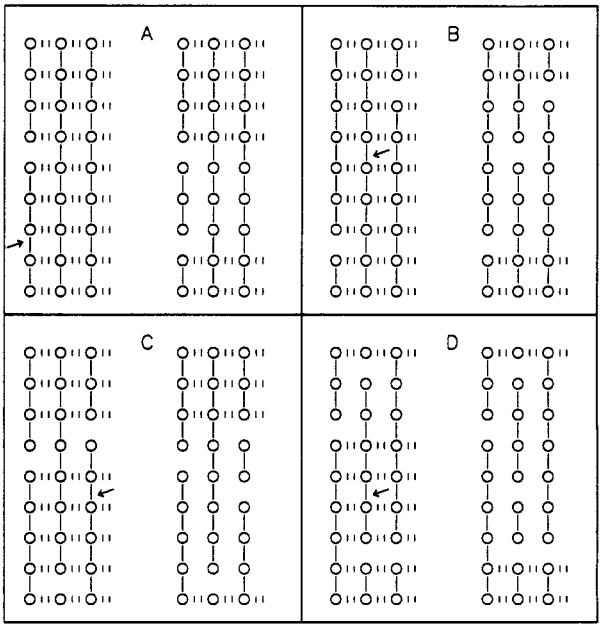

Figure 6. Schematic illustration of the consequences of cleavage (arrow) of a glycosidic linkage in one of the strands in a triple-stranded species: scission of one linkage resulting in two species either by release of an oligosaccharide shorter than DP_{min} (A) or by scission of the triple strand when a neighboring preexisting nick is less than DP_{min} apart (B), and scission resulting in three and four independent species by simultaneous release of one and two oligosaccharide and triple-strand scission C and D, respectively). $DP_{min} = 3$ was assumed in this illustration.

(Figure 4) suggest that ν_2 can be used to obtain information about strandedness. The exponent ν_2 correlates to the number of strands (m) as $\nu_2 = 0.35 + 0.66m$ for these three homogeneous cases. Information about heterogeneity in strandedness, i.e., partly double or triple strandedness, is therefore potentially accessible based on interpolation

between these homogeneous cases.

Comparison to Experiments. The three features of the model preditions that can be tested experimentally are, first, the enhanced stability in the initial degradation, second, the exponents ν_2, and, third, the release of low molecular weight material.

The apparently retarded depolymerization for $t_r < t_{r,ind}$ is due to the ability to mask effects of scission in one of the polymer chains. Experiments suggesting that stabilization occurs in the ordered conformation of xanthan are reported by Milas and Rinaudo.[45] They exposed a xanthan sample while kept in the ordered conformation to mild acid hydrolysis. No change in the relative viscosity, η_{rel}, determined for the order conformation was observed. Subsequently, they heated the sample toward the melting temperature, T_m, of the ordered conformation and cooled. When heated to or above T_m, they observed a substantial, irreversible decrease in η_{rel}, as well as a reduction in M_w. The ordered conformation is therefore able to mask broken glycosidic linkages. Exposing such samples to disordering conditions discloses a preexisting scission, and the structure separates into its individual parts.

Analogous changes in molecular weight occurring in a order–disorder–order cycle are also reported for xanthan samples not deliberately subjected to degrading conditions.[46-48] Evidence from such "dissociation experiments" suggests that the initial stabilization reported in the acid-catalyzed accelerated depolymerization[18] and the difference in thermal stability between the ordered and disordered conformation are due to the double-stranded nature of the ordered conformation. Differences in catalytic activity toward cleavage of glycosidic linkages in the two conformations are not necessary to account for the observations but cannot be ruled out.

The length of the induction period can be used for the experimental determination of DP_{min} as reported for DNA by Thomas[19] provided that the fraction of broken glycosidic linkages is known. Most of the thermal stability studies on xanthan report properties that reflect an apparent molecular weight, and no direct information on the fraction of broken glycosidic linkages is determined. Correlation between reported experimental data and the present simulations to establish DP_{min} under the condition of degradation is therefore not possible. Likewise, the independence of ν_2 on DP_{min} (Figure 4B) does not allow an alternative route to establish DP_{min}.

The power law region, fully developed for reductions in M_w of 80% and larger, represents a prediction which can be tested experimentally. Figure 7 shows the experimental data for acid-catalyzed hydrolysis of ordered xanthan reported by Christensen and Smidsrød.[18] Also shown are model predictions of xanthan for $DP_{min} = 4$ shifted along the axes to facilitate comparison of the region $t_r > t_{r,ind}$. The data initially obtained as the intrinsic viscosity, $[\eta]$, were converted to DP using the experimentally determined relationship between M_w and $[\eta]$.[22] There is good agreement between the exponent from the experimental data, 1.5 ± 0.1, and that from the model predictions (Figure 7). The experimental finding that $\nu_2 = 1.5 \pm 0.1$ supports a double-stranded structure for the acid form of the polymer in line with other conclusions.[49] Most reported studies on the thermal stability of xanthan in the ordered conformation do not include the region where less than 20% of the initial M_w remains with sufficient resolution to allow a detailed comparison to the predicted exponent ν_2.

The predicted release of oligomers during depolymerization of xanthan in the ordered conformation is suitable for experimental testing of the model. Such experiments

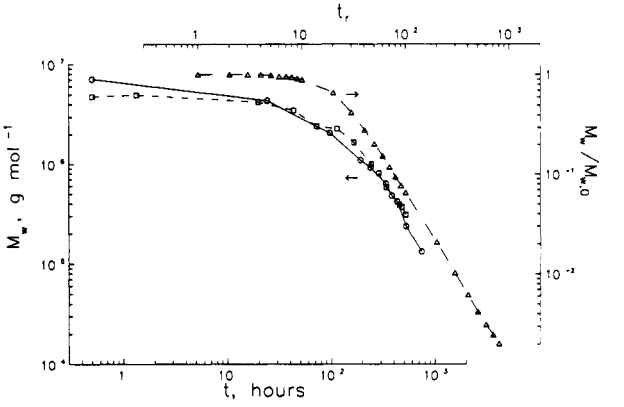

Figure 7. log $M_w/10^6$ versus log t/h for acid-catalyzed depolymerization of xanthan in the ordered conformation: (□) pH 3, ionic strength 500 mM; (○) pH 2, ionic strength 500 mM. log $(M_w/M_{w,0})$ versus log t_r for Monte Carlo simulation of xanthan degradation assuming $DP_{min} = 4$ (△). The x and y axes of the simulation were shifted to facilitate comparison of the power law regime.

could address distributions of DP_{min} at various temperatures relative to T_m. The reported truncation of the side chains releasing mono-, di-, and trisaccharides during depolymerization[18] makes the interpretation of the released oligomer distribution of such comblike polymers more complex. In addition, we are not aware of any analysis of this aspect of depolymerizing xanthan and will therefore not pursue this aspect further. However, release of low molecular weight fragments is reported to occur under depolymerization of the duplex-DNA,[50,51] suggesting that similar observations would not be unexpected in xanthan.

The computations predict a prolonged induction period followed by a power law region with exponent 2.3 when going from the double- to the triple-stranded polymer. There are fewer reports on the thermal stability of scleroglucan than xanthan. Davison and Mentzer[2] report that the viscosity loss of aqueous scleroglucan solutions is smaller than that for xanthan solutions aged at 90 °C. They also report differences in the thermal stability among scleroglucan products, with aqueous broths being superior to dried and subsequently dissolved ones. The enhanced thermal stability of scleroglucan compared to that of xanthan can be accounted for in terms of the predicted prolonged induction period when going from the double- to the triple-stranded polymer (compare parts A and B of Figure 3). However, differences in the stability of the two different types of glycosidic linkages (β-(1→3) and β-(1→4) for scleroglucan and xanthan, respectively) cannot be ruled out. Detailed molecular studies of the degradation of scleroglucan addressing this prediction are currently carried out in this laboratory.

Implications for Use of "Viscosity Decay" Models in Polymer Flooding Simulations. Simulations of polymer flooding of oil reservoirs have in recent years been extended to include potential effects of polymer degradation.[52] The degradation process is implemented to a first approximation using first-order kinetics of the effective polymer concentration. The results from the present calculations suggest that such use of a single-exponential decay to describe degradation is not correct for double- and triple-stranded polymers. In Figure 8 we have compared the decrease in the molecular weight in a first-order reaction with the results for the simulations of double- and triple-stranded polymers using $DP_{min} = 4$ assuming identical half-lives $t_{1/2}$ (time for reduction to 50% of the initial M_w) for the three types of depolymerization. This figure illustrates that the single-expo-

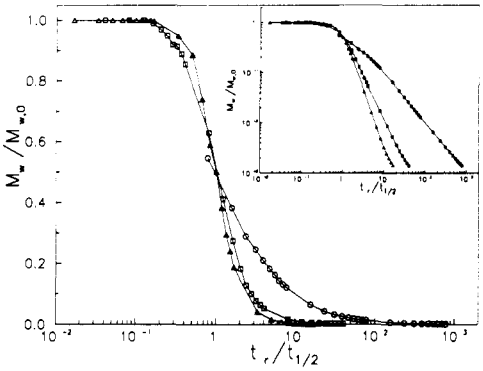

Figure 8. Predicted $M_w/M_{w,0}$ versus $t_r/t_{1/2}$ for depolymerization of double- (□) and triple-stranded (△) polymers compared with that of a single-stranded polymer (○).

nential decay description underestimates M_w compared to the more elaborated prediction for $t_r < t_{1/2}$. The overestimate in M_w for $t_r > t_{1/2}$ appears to be of a small absolute value (on the linear scale) but appears larger on a relative scale (Figure 8, inset). The overestimate in M_w is about a factor 4 and 11 at $5t_{1/2}$ for the double- and triple-stranded case, respectively. For the polymer flooding operation where incremental oil recovery due to the addition of polymer is expected to occur several half-lives after the polymer slug injection is started, the differences in depolymerization kinetics could be influential on the predictions. Incorporation of the detailed depolymerization kinetics of multistranded biopolymers may represent one way to improve the polymer flooding simulators and thereby increase the confidence of such predictions.

Acknowledgment. This work was supported by VISTA, a research cooperation between the Norwegian Academy of Science and Letters and Statoil, and by the Royal Norweigian Council for Scientific and Industrial Research (NTNF).

References and Notes

(1) Ryles, R. G. *SPE Reservoir Eng.* **1988**, *Feb*, 23.
(2) Davison, P.; Mentzer, E. *SPEJ, Soc. Pet. Eng. J.* **1982**, *June*, 353.
(3) Ash, S. G.; Clarke-Sturman, A. J.; Calvert, R.; Nisbet, T. M. Presented at the 58th Annual Conference and Exhibition of the Society of Petroleum Engineers, San Francisco, CA, Oct 5–8, 1983.
(4) Seright, R. S.; Henrici, B. J. Presented at the SPE/DOE Fifth Symposium on Enhanced Oil Recovery of the Society of Petroleum Engineers and the Department of Energy, Tulsa, OK, Apr 20–23, 1986.
(5) Hatakenaka, K.; Liu, W.; Norisuye, T. *Int. J. Biol. Macromol.* **1987**, *9*, 346.
(6) Milas, M.; Linossier, J. L.; Contat, F. *J. Appl. Polym. Sci.* **1988**, *35*, 1115.
(7) Kierulf, C.; Sutherland, I. W. *Carbohydr. Polym.* **1988**, *9*, 185.
(8) Lund, T.; Lecourtier, J.; Muller, G. *Polym. Degrad. Stab.* **1990**, *27*, 211.
(9) Wellington, S. L. *SPEJ, Soc. Pet. Eng. J.* **1983**, *Dec*, 901.
(10) Wellington, S. L. U.S. Patent 4,218,327, 1980.
(11) Chen, C. S. H.; Sheppard, E. W. *J. Macromol. Sci., Chem.* **1979**, *A13*, 239.
(12) Bragg, J. R.; Maruca, S. D.; Gale, W. W.; Gall, L. S.; Wernau, W. C.; Beck, D.; Goldman, I. M.; Laskin, A. I.; Naslund, L. A. Presented at the 58th Annual Conference and Exhibition of the Society of Petroleum Engineers, San Francisco, CA, Oct 5–8, 1983.
(13) O'Leary, W. B.; Boivin, J. W.; Dasinger, B. L.; Beck, D.; Goldman, I. M.; Wernau, W. C. *SPE Reservoir Eng.* **1987**, *Nov*, 647.
(14) Lambert, F.; Rinaudo, M. *Polymer* **1985**, *26*, 1549.
(15) Foss, P.; Stokke, B. T.; Smidsrød, O. *Carbohydr. Polym.* **1987**, *7*, 421.
(16) Stokke, B. T.; Elgsaeter, A.; Smidsrød, O. *Int. J. Biol. Macromol.* **1986**, *8*, 217.
(17) Liu, W.; Sato, T.; Norisuye, T.; Fujita, H. *Carbohydr. Res.* **1987**, *160*, 267.
(18) Christensen, B. E.; Smidsrød, O. *Carbohydr. Res.* **1991**, *214*, 55.
(19) Thomas, C. A. *J. Am. Chem. Soc.* **1956**, *78*, 1861.
(20) Hagen, U. *Biochim. Biophys. Acta* **1967**, *134*, 45.
(21) Paradossi, G.; Brant, D. A. *Macromolecules* **1982**, *15*, 874.
(22) Sato, T.; Norisuye, T.; Fujita, H. *Polym. J.* **1984**, *16*, 341.
(23) Sato, T.; Kojima, S.; Norsiyue, T.; Fujita, H. *Polym. J.* **1984**, *16*, 423.
(24) Sato, T.; Norisuye, T.; Fujita, H. *Macromolecules* **1984**, *17*, 2696.
(25) Coviello, T.; Kajiwara, K.; Burchard, W.; Dentini, M.; Crescenzi, V. *Macromolecules* **1986**, *19*, 2826.
(26) Stokke, B. T.; Elgsaeter, A.; Smidsrød, O. *ACS Symp. Ser.* **1989**, *396*, 145.
(27) Paoletti, S.; Cesaro, A.; Delben, F. *Carbohydr. Res.* **1983**, *123*, 173.
(28) Norton, I. T.; Goodall, D. M.; Frangou, S. A.; Morris, E. R.; Rees, D. A. *J. Mol. Biol.* **1984**, *175*, 371.
(29) Holzwarth, G.; Ogletree, J. *Carbohydr. Res.* **1979**, *76*, 277.
(30) Shatwell, K. P.; Sutherland, I. W.; Ross-Murphy, S. B. *Int. J. Biol. Macromol.* **1990**, *12*, 71.
(31) Shatwell, K. P.; Sutherland, I. W.; Dea, I. C. M.; Ross-Murphy, S. B. *Carbohydr. Res.* **1990**, *206*, 87.
(32) Liu, W.; Norisuye, T. *Int. J. Biol. Macromol.* **1988**, *10*, 44.
(33) Yanaki, T.; Tabata, K.; Kojima, T. *Carbohydr. Polym.* **1985**, *5*, 275.
(34) Kitamura, S.; Kuge, T. *Biopolymers* **1989**, *28*, 639.
(35) Yanaki, T.; Ito, W.; Tabata, K.; Kojima, T.; Norisuye, T.; Takano, N.; Fujita, H. *Biophys. Chem.* **1983**, *17*, 337.
(36) Zimm, B. H. *J. Chem. Phys.* **1960**, *33*, 1349.
(37) Applequist, J.; Damle, V. *J. Am. Chem. Soc.* **1965**, *87*, 1450.
(38) Shibata, J. H.; Schurr, J. M. *Biopolymers* **1981**, *20*, 525.
(39) Higgs, P. G.; Ball, R. C. *J. Phys. Fr.* **1989**, *50*, 3285.
(40) Zimm, B. H.; Bragg, J. K. *J. Chem. Phys.* **1959**, *31*, 526.
(41) Hacche, L. S.; Washington, G. E.; Brant, D. A. *Macromolecules* **1987**, *20*, 2179.
(42) Jansson, P. E.; Kenne, L.; Lindberg, B. *Carbohydr. Res.* **1975**, *45*, 275.
(43) Johnson, J.; Kirkwood, S.; Misaki, A.; Nelson, T. E.; Scoletti, J. V.; Smith, F. *Chem. Ind. (London)* **1963**, 820.
(44) Tanford, C. *Physical Chemistry of Macromolecules*; John Wiley & Sons, Inc.: New York, 1961.
(45) Milas, M.; Rinaudo, M. *Carbohydr. Res.* **1986**, *158*, 191.
(46) Lecourtier, J.; Chauveteau, G.; Muller, G. *Int. J. Biol. Macromol.* **1986**, *8*, 306.
(47) Muller, G.; Lecourtier, J. *Carbohydr. Polym.* **1988**, *9*, 213.
(48) Lange, E. A. In *Water-Soluble Polymers for Petroleum Recovery*; Stahl, G. A., Schulz, D. N., Eds.; Plenum Press: New York, 1988; pp 231–241.
(49) Zhang, L.; Liu, W.; Norisuye, T.; Fujita, H. *Biopolymers* **1987**, *26*, 333.
(50) Sinsheimer, R. L. *J. Biol. Chem.* **1953**, *208*, 445.
(51) Zamenhof, S.; Chragaff, E. *J. Biol. Chem.* **1950**, *187*, 1.
(52) Clifford, P. J.; Sorbie, K. S. Presented at the International Symposium on Oilfield and Geothermal Chemistry of the Society of Petroleum Engineers, Phoenix, AZ, Apr 9–11, 1985.

Registry No. Xanthan, 11138-66-2; scleroglucan, 39464-87-4.